Instrument Science Report WFC3 2013-12

WFC3 Post-Flash Calibration

J. Biretta and S. Baggett
June 27, 2013

ABSTRACT

We review the Phase II implementation of the WFC3/UVIS post-flash capability, as well as its GO science utilization in Cycle 20. With details of the GO usage in mind, calibration proposals were written to provide data for study and calibration of the post-flash capability. We confirm the illumination pattern is relatively uniform; broad patterns are present with +/-20% brightness variations. Stacking a large number of FLASH=12 images reveals numerous traps and interesting features comprised of bright single pixels with dark tails. Highly exposed flash images (~7000 e-/pixel) show small numbers of few-pixel dust spots, scratches, and other normal CCD features at the 10% to 30% level. Flash images obtained on the A and B shutters are very similar -- the flashes are about 7% fainter on shutter B vs. shutter A, and the ratio of shutter A / shutter B shows a smooth ~4% gradient running across the field of view from amplifier A to amplifier D. The total counts/pixel appear to be non-linear with flash duration for both the LOW and MEDIUM current settings -- both settings run about 8% brighter at short flash durations as compared to 100 sec durations. We discuss the data headers, CALWF3, and pipeline implementations of post-flash calibration. Calibration reference files were derived in both shutters for the LOW and MEDIUM current settings with un-binned pixels. These have been extensively tested and delivered to CDBS. Examination of the long-term stability of the LED shows no evidence of systematic fading over 9 months, but finds quasi-random brightness fluctuations with an RMS ~1.2%. We see no evidence for long-term changes in the spatial illumination pattern exceeding ~0.1%.

Introduction

The WFC3/UVIS channel CCDs suffer from charge transfer efficiency problems, as do all past and present CCDs on-board HST. Radiation bombardment from the harsh space environment causes trapping sites to appear in the CCD over time. These gradually grow in number, and eventually rob images of significant counts (electrons) during readout of the image. This leads to a reduction in photometric counts, and a potential loss of faint targets, especially in regions far from the readout amplifier. A successful mitigation strategy is to flash the CCDs with a diffuse light source prior to readout, so as to raise the overall background of the image. This has the effect of filling trapping sites, and hence preserving more of the electrons which comprise the image. However, flashing is not a complete cure -- some electrons are still lost, and the overall background noise of the image is increased. [1]

With this possibility in mind, a flash capability was built into WFC3 whereby the CCD side of the shutter can be illuminated by a single LED just prior to readout (i.e. post-flashing the image). This provides a highly diffuse light, which uniformly illuminates the CCDs. Pre-launch ground tests of the post-flash capability have verified the illumination is uniform to about +/- 20%, and appears to be relatively stable from image to image (Baggett and Wheeler, 2012).

Initial on-orbit tests of the post-flash capability (Anderson, et al., 2012) have shown it to be highly effective in mitigating CTE effects in typical science images. In particular, they find the "sweet-spot" for reducing CTE effects in the WFC3 CCDs occurs at image backgrounds (natural + flash) ~12 e-/pixel. This is shown to reduce CTE losses for low S/N targets from 90% to 15%. The electrons per pixel generated by the flash can be controlled by adjusting both the lamp current (LOW, MEDIUM, and HIGH settings) and the lamp on-time.

Herein we summarize the implementation of the WFC3/UVIS post-flash capability both in terms of observation planning (i.e. phase II) and post-observation calibration (CALWF3). We survey the Cycle 20 post-flash utilization by observers, and with this in mind, have created several observing programs to study and calibrate the post-flash capability. We examine the general properties of the post-flash, and create reference files for use in the calibration pipeline. Finally we study the long- and short-term stability of the post-flash, and outline areas needing additional work in the future.

[1] The noise increase is simple Poisson noise associated with the increased illumination from the flash. An alternate strategy to flashing is to correct the image photometry post-observation using a model of CTE effects. However, such models cannot recover lost targets, and ultimately the best results may come from a combination of flashing and post-observation correction.

Phase II Implementation

The WFC3 post-flash capability was first implemented in Cycle 19. Initially it was available only through phase II "engineering only" Special Requirement QESIPARMs. The lamp current was controlled by specifying the Special Requirement "QESIPARM FLASHCUR [value]" where [value] could be LOW, MEDIUM, or HIGH. The lamp on-time could be specified by "QESIPARM FLASHEXP [time]" where the time is give in seconds with a resolution of 0.1 sec.

Later in Cycle 20 a simpler post-flash implementation was created for the use of observers where they specify the desired flash level in e-/pixel using the phase II Optional Parameter "FLASH=[value]" where integer values 0 to 25 are supported. The FLASH level is the approximate image background in e-/pixel added by the post-flash. These are then executed using the duration and current settings listed in Table 1. Non-standard flashes can also be commanded using the "engineering only" Optional Parameters FLASHCUR and FLASHDUR with values similar to the Cycle 19 QESIPARMs described in the previous paragraph.

The post-flash does require a small additional overhead time, which is roughly equal to the lamp on "duration" listed in Table 1. (Since the post-flash is performed by illuminating the closed shutter, it cannot be done simultaneously with the science exposure.) We note that FLASH=15 and FLASH=22 use the MEDIUM current setting which produces higher illumination, and hence these require less overhead time as compared to the LOW current setting. The flash count rate is roughly 29 times higher for the MEDIUM current as compared to the LOW current setting, and hence the lamp on-times are much shorter. [2]

Calibration exposures for the post-flash must be implemented as dark frames with TARGET=DARK. There is no specific capability to take post-flashed bias frames on-orbit, so these are commanded as 0.5 sec dark frames (which is the minimum allowable exposure time for dark frames).

[2] The count rate for the HIGH current setting is only ~12% higher than the MEDIUM current setting (for FLASHDUR=2.5 sec). It does not offer any unique capabilities, hence it has not been fully supported nor calibrated so far.

Table 1. Phase II FLASH levels and corresponding settings.

Phase II FLASH Level (e-/pixel)	Duration (sec)	Current
1	0.4	LOW
2	0.8	LOW
3	1.2	LOW
4	1.6	LOW
5	2.0	LOW
6	2.3	LOW
7	2.7	LOW
8	3.1	LOW
9	3.5	LOW
10	3.9	LOW
11	4.3	LOW
12	4.7	LOW
13	5.0	LOW
14	5.4	LOW
15	0.2	MEDIUM
16	6.2	LOW
17	6.6	LOW
18	7.0	LOW
19	7.3	LOW
20	7.7	LOW
21	8.1	LOW
22	0.3	MEDIUM
23	8.9	LOW
24	9.3	LOW
25	9.7	LOW

Cycle 20 GO Science Observations

In an effort to better understand the needs of the observer community, we analyzed the Cycle 20 phase II proposals in late July 2012, i.e. shortly after the Cycle 20 phase II deadline. We obtained a listing of all the requested phase II exposures for Prime Target GO observations from Merle Reinhart. The requested values of FLASH are displayed as a histogram in Figure 1. Roughly 2/3 of the exposure log sheet lines did not request post-flash, and presumably

these are long exposures in broad- and medium-band filters where the natural sky background is sufficient to mitigate CTE effects. The remaining 1/3 of the requested exposure log sheet lines did request post-flash, and of these the vast majority use FLASH=8. Other popular values are FLASH=5, 10, and 20. Remaining values used by observers are FLASH=3, 7, 9, 11, 12, and 15. We note that this plot shows the number of exposure log sheet lines, and is likely to be different from the number of exposures due to dither patterns, CR-SPLITs, and repetitions. Nonetheless it provides a useful picture of the observer requests for post-flash.

Nearly all flashed observations are using the LOW current setting. Only one proposal, program ID 12899, used FLASH=15 which utilizes the MEDIUM current setting (Table 1). This program was scheduled to execute around April 16, 2013.

Binning is another interesting parameter to consider when planning post-flash calibrations. The vast majority of the planned observations use the default un-binned mode. Only one program requested binned data, program ID 12879, which requested BIN=2 and FLASH=10. Their exposures begin in July 2012 and run through Cycle 20. We discussed their calibration needs with these observers, and they indicated they were planning to create their own calibration reference files, hence making our work less urgent. Binning was typically used in the past to reduce read-noise in situations where read-noise dominates the image noise. However, the recommended flash levels are such that the post-flash will dominate the noise, and hence we do not anticipate very many science images with both binning and post-flash.

We note that these represent only the initial phase II submissions in July 2012; it is likely that some programs were modified at a later date.

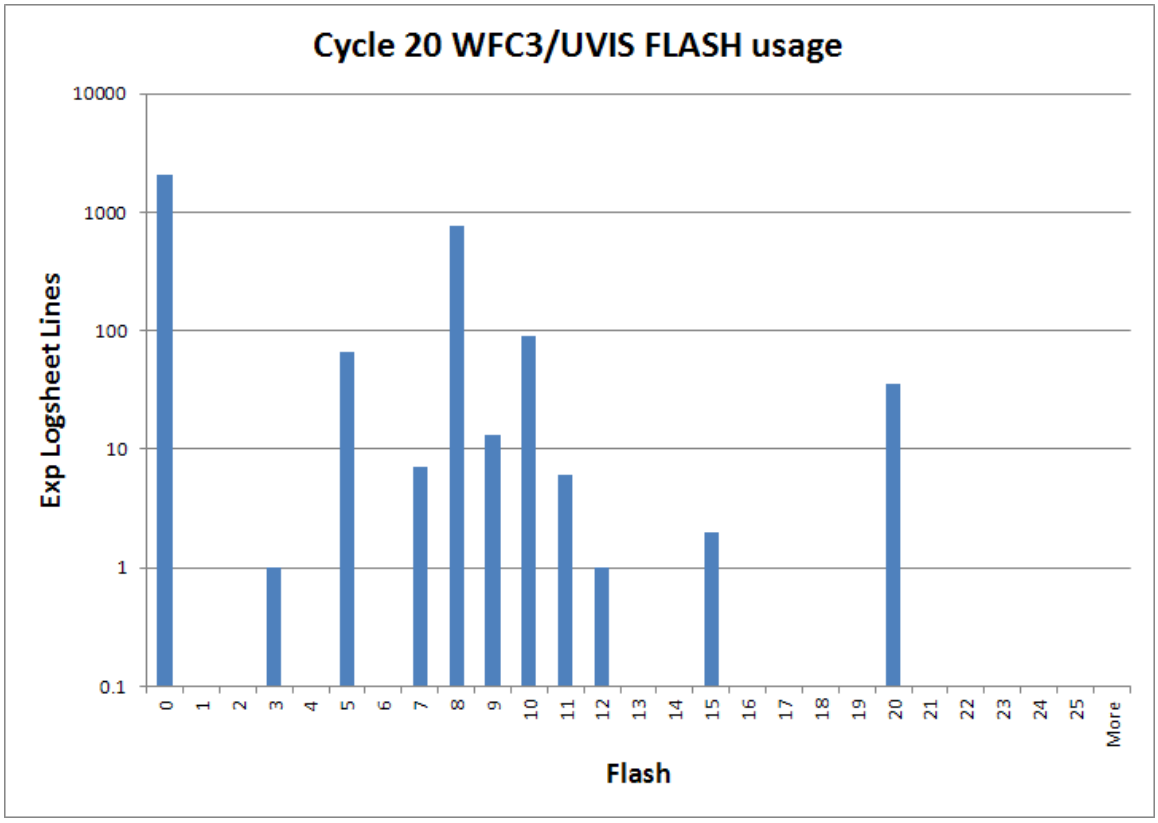

Figure 1. Histogram showing the number of exposure log sheet lines requesting each FLASH value for Cycle 20 GO Prime Targets as of late July 2012.

Calibration Proposals

The calibration proposals are listed in Table 2. The first program, 12802, acted as an on-orbit commissioning of the post-flash capability, and executed between May and July 2012. Images are taken with a variety of flash durations in the MEDIUM current setting to map-out the resulting image background levels. Smaller numbers of images are also taken in the LOW and HIGH current settings for similar purposes. Medium length (360 sec) dark frames are obtained at a range of post-flash levels to help validate CTE models. Observations of stellar fields in NGC104 and Omega Cen are taken with and without post-flash to test its efficacy in mitigating CTE losses.

Program 13069 is an ad-hoc program designed to provide early calibration of science observations obtained with post-flash late in Cycle 19 and in Cycle 20. The program was assembled from unused orbits in other Cycle 19 calibration programs. It has a diverse set of goals which includes calibration of GO science data, production of pipeline reference files, characterization of CTE effects for various flash levels, and dark calibration for

contemporary flashed science observations. The observations are primarily made with the LOW current setting, which is utilized by the majority of FLASH values available to observers (Table 1) and was also used by the vast majority of Cycle 20 observers who flashed their data. Bias[3] and dark frames (900 sec) are obtained with the 12 e-/pixel flash which is recommended to observers. Short darks (100 sec) are obtained with background levels from 0 to 105 e-/pixel to study CTE mitigation as a function of background (these might potentially be used to constrain pixel-based CTE corrections). Highly exposed flash images (~7000 e-/pixel) are obtained to provide high signal-to-noise ratio images as ingredients to pipeline reference files; these are obtained with both shutters.[4] Flash images are also obtained in 3x3 binned mode to test for any issues related to binning. The program executed between August and October 2012.

Program 13078 looks for changes in the post-flash calibration. Full-frame dark images are obtained with FLASH=12 and as well as very bright flashes (~7000 e-/pixel using FLASHCUR=MED, FLASHDUR=100) to test for changes in the brightness distribution of the post-flash image. Additional images are obtained at FLASH values used by science observations (Figure 1) to monitor lamp brightness; these are taken with the C1K1C sub-array to minimize readout times. The program executes monthly beginning in November. 2012 and runs through November 2013.

The UVIS Daily Monitor Programs (programs 13073-13076) contain a large number of full-frame bias images with FLASH=12 to test the stability of the bias and post-flash calibration. This program runs from November 2012 to November 2013.

Table 2. Calibration proposals.

Program ID	Title	PI	Cycle	Orbits Allocated
12802	WFC3 Post-Flash Characterization	J. Mackenty	19	20
13069	WFC3 UVIS Post-Flash Calibration	J. Biretta	19/20	99
13078	UVIS Post-Flash Monitor	J. Biretta	20	64
13073-13076	UVIS Daily Monitor	J. Biretta	20	805

[3] Post-flashed bias frames are commanded as 0.5 sec dark frames.

[4] The shutter is toggled using a brief TUNGSTEN sub-array exposure.

General Properties of the Post-flash

A typical FLASH=12 post-flash in shutter A is displayed in Figure 2. The image is a 0.5 sec full-frame dark, it has been bias and dark calibrated in CALWF3, and then scaled by the gain of 1.56 e-/DN to convert to e-/pixel. The local mean level (measured with IMSTAT) ranges from ~10.3 e-/pixel near the C amplifier to a maximum ~15.2 e-/pixel near the amp B/D border (x,y) = (2700,2200). The large-scale non-uniformity in the post-flash brightness is hence +/-19%. The RMS noise in the brightest region is 5.1 e-/pixel, which is close to the expected combination of read noise and post-flash photon noise of 4.9 e-/pixel.

Figure 3 shows the result of averaging 24 of these images (0.5 sec darks with FLASH=12) with cosmic ray rejection. The noise is reduced and the illumination pattern is more apparent. Two interesting types of features appear in this image. The first are numerous dark pixels, with many having dark tails that extend a few pixels in the +y direction (Figure 4 and Figure 5). The dark pixels have values as low as 1 e-/pixel, with many having values or 4 to 6 e-/pixel. These are consistent with charge-trapping sites. The other interesting feature is numerous bright pixels with dark tails. These tend to appear at low y values on the CCD (i.e. near the readout amplifier). Many of these bright pixels have values roughly twice that of normal pixels, as if they contain the sum of a normal charge and that of the pixel immediately above it. Both these features are caused by defects in the CCD, and underscore the importance of dithering science observations.

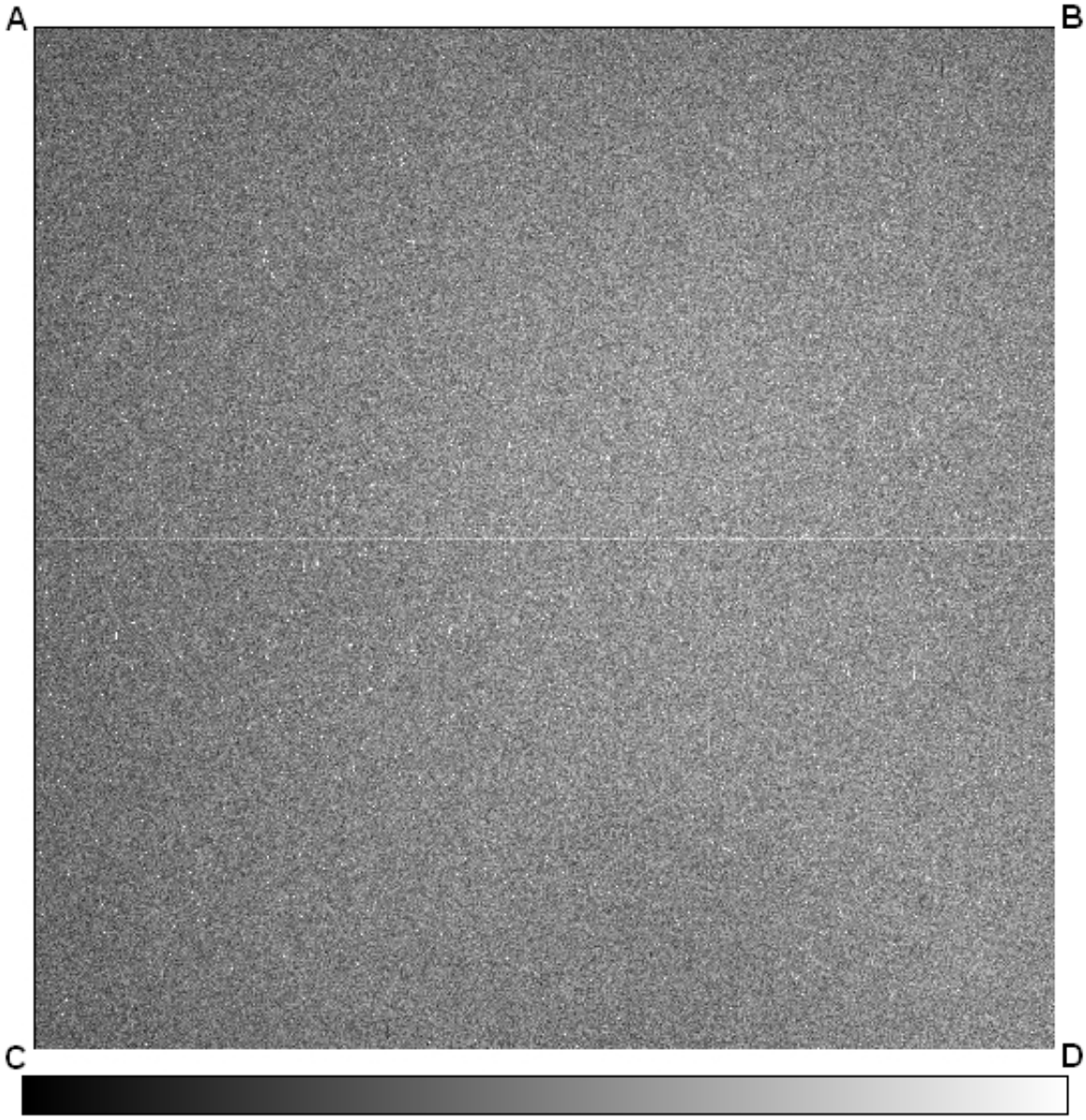

Figure 2. Image ic3m06mwq from proposal 13069 showing a typical FLASH=12 post-flash on shutter A applied to a 0.5 sec full-frame dark. The brightness scale runs from 0 to 25 e-/pixel. The locations of the four amplifiers are labeled A, B, C, and D. Cosmic rays have not been removed.

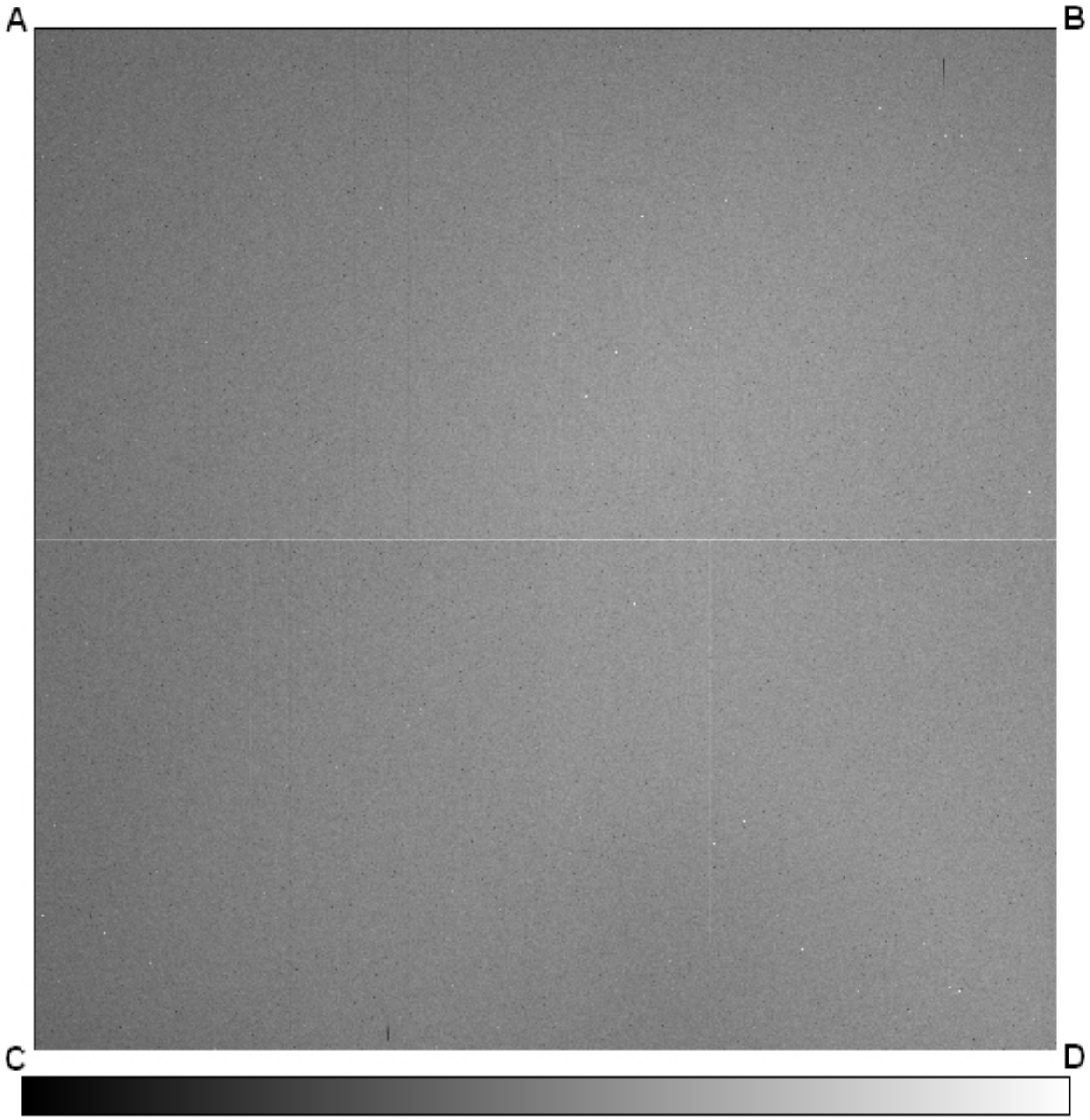

Figure 3. Average of all 24 full-frame 0.5 sec darks post-flashed with FLASH=12 on shutter A from proposal 13069. The brightness scale runs from 0 to 25 e-/pixel. The locations of the four amplifiers are labeled A, B, C, and D. Cosmic rays have been removed with STSDAS CRREJ.

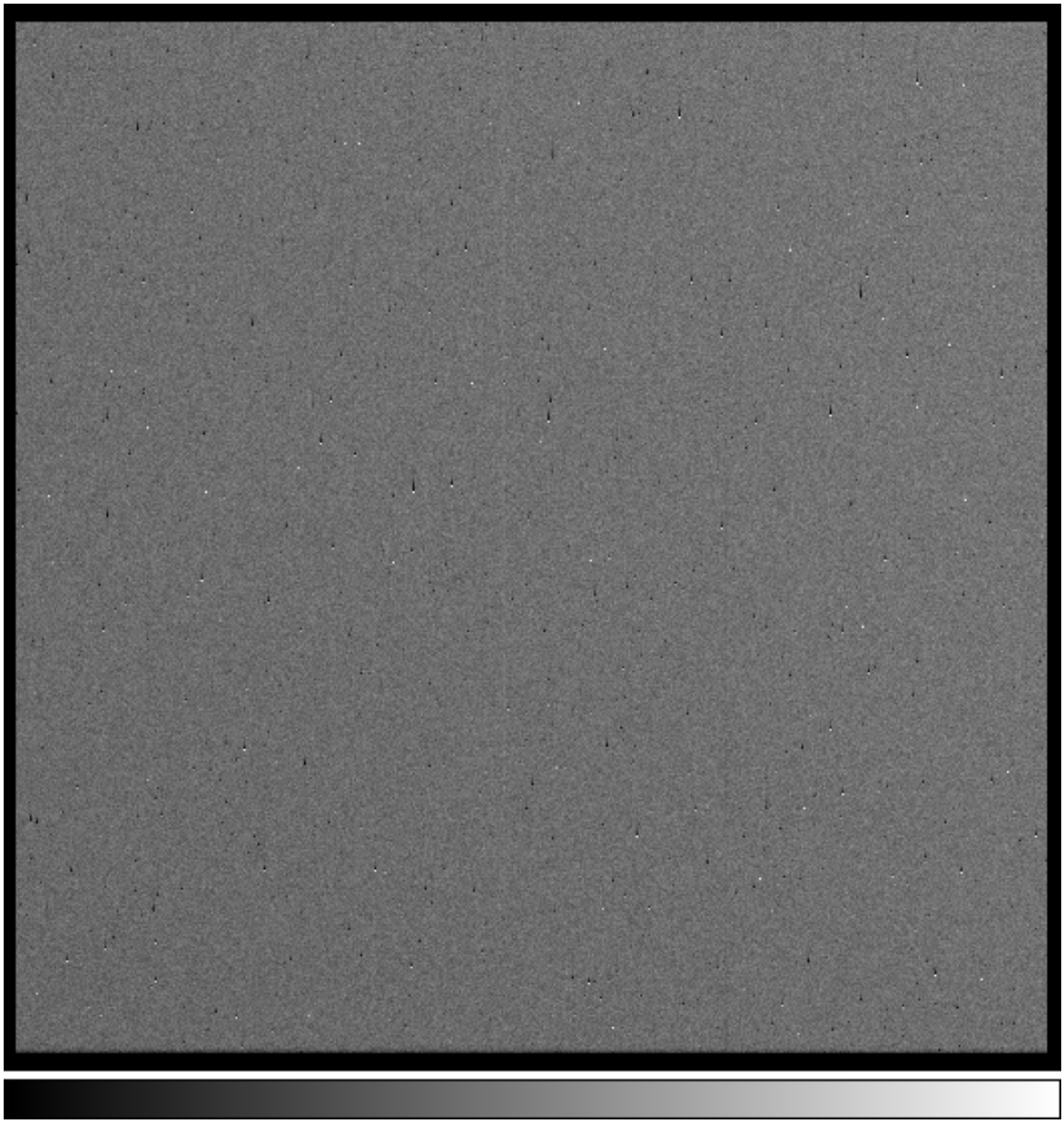

Figure 4. Detail of Figure 3 showing the 512x512 pixel region closest to amplifier C (which is at lower left). Numerous bright and dark pixels are seen with dark tails. The brightness scale runs from 0 to 25 e-/pixel.

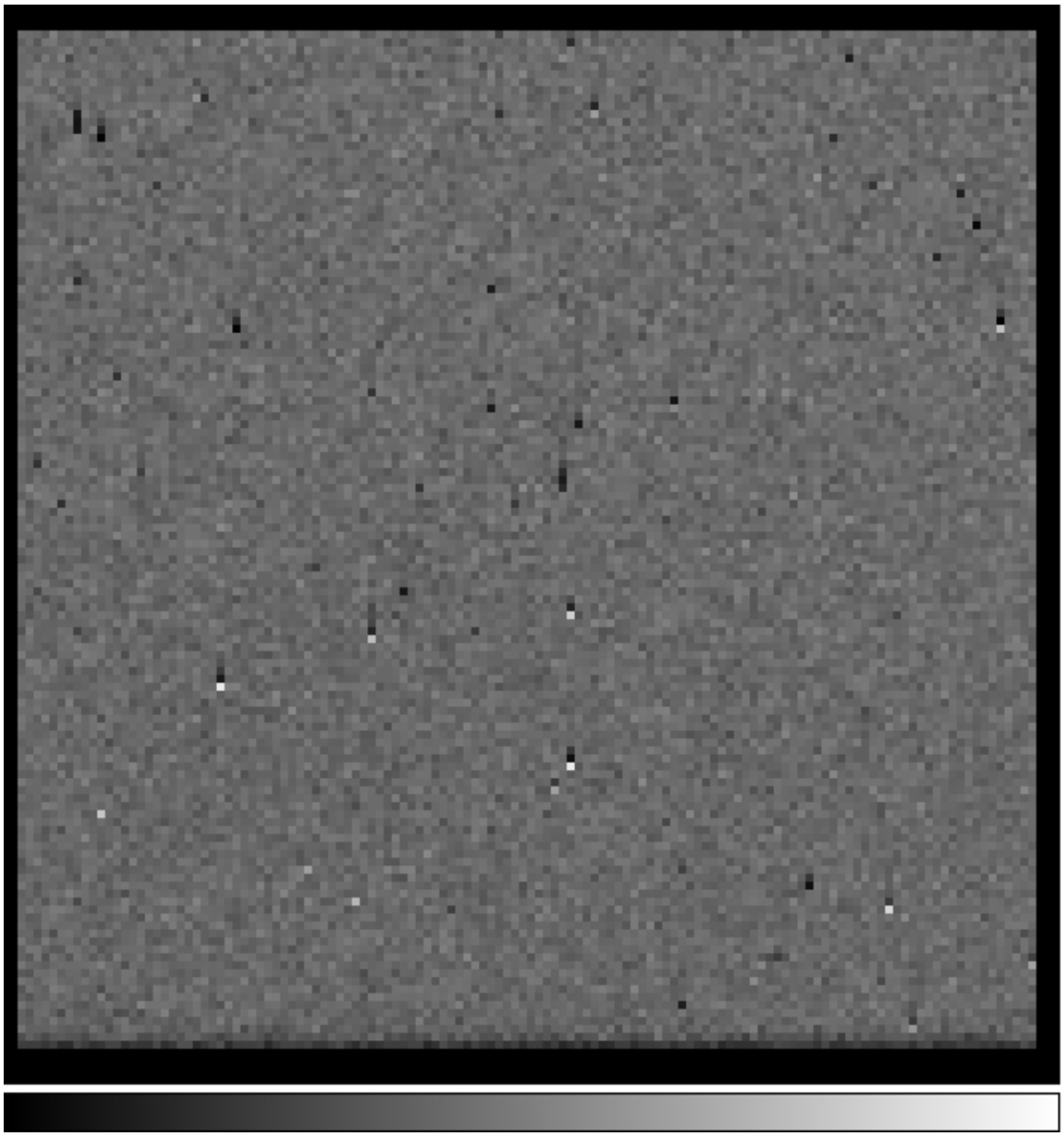

Figure 5. Detail of Figure 3 showing the 128x128 pixel region closest to amplifier C (which is at lower left). Bright single pixels are seen with dark tails. Many dark pixels with tails, presumably charge traps, are also visible. The brightness scale runs from 0 to 25 e-/pixel.

The structure of the post-flash for very bright flashes is illustrated in Figure 6. This shows the average of four images (with cosmic ray rejection and dark subtraction) with FLASHCUR=MED and FLASHDUR=100 sec. This is one of the images that will later be used in generating the reference files, so it is interesting to examine its structure. The brightness range of the image runs from ~5900 e-/pixel near amplifier C, to ~8900 e-/pixel

near (x, y) = (2500, 2350). The brightness range is +/-20%, similar to that seen in Figure 2 and Figure 3 for low-brightness flashes. Besides the very broad intensity gradients, there are faint arcs and wisps visible throughout the field at the ~0.5% to ~1% level. A pair of narrow dark lines are visible crossing quadrants A and B; these are about 10% deep and are scratches (manufacturing defects) on the surface of the CCD. Several tiny black spots are also visible that are ~30% deep; some of these are a few pixels in diameter and are likely to be dust spots, while others are confined to a single column on the CCD and may be some sort of charge trap defect. A few lithographic defects are also visible – these are slightly dark vertical columns spanning one or both of the two CCDs. [5]

Figure 7 shows a detail of Figure 6 image near the border between the A and B quadrants. The two scratches are visible, along with several scattered dust spots. A blocked column appears at the lower right as a very dark vertical line. A dark vertical lithographic error is visible on the right spanning the entire height of the figure, and a bright horizontal lithographic error is visible near the bottom spanning the entire width of the figure.

Figure 8 shows a 128 x 128 pixel detail of the region nearest the C amplifier taken from Figure 6. The image is nearly devoid of any features. We previously saw many bright and dark trap-like features in an averaged FLASH=12 image for this same region (Figure 5). As expected, the traps only effect faint count levels, and are completely invisible at this highly exposed flash image (~7000 e-/pixel)..

[5] Lithographic defects are manufacturing errors where vertical columns and/or horizontal rows are slightly too narrow or too wide, and hence appear dark or bright relative to normal columns and rows.

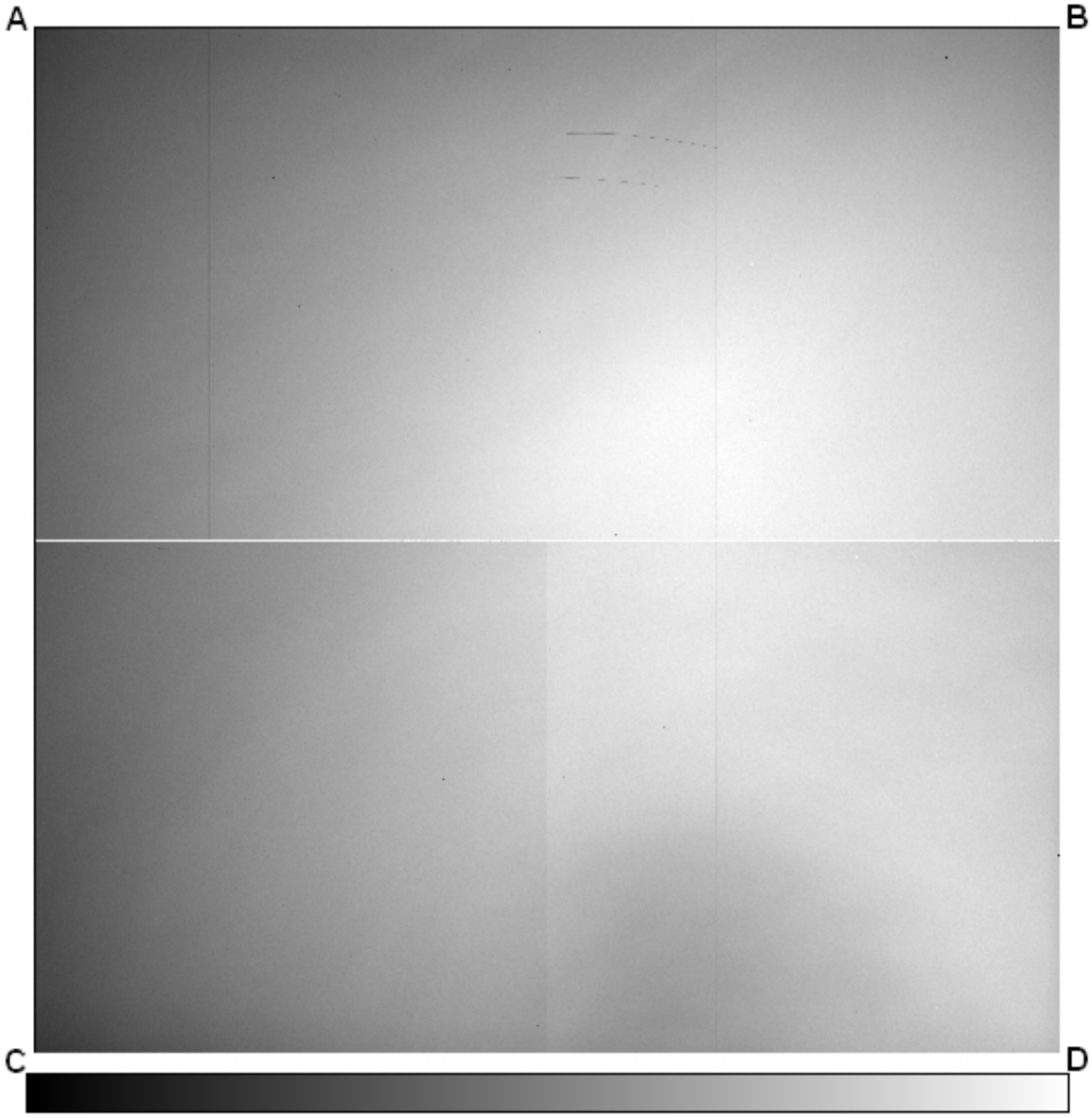

Figure 6. Average of four very bright flashes obtained as 0.5 sec dark frames with FLASHCUR=MED and FLASHDUR=100 sec in shutter A from proposal 13069. (See Table 4 for image names.) The images were combined with STSDAS CRREJ, and the dark current was removed using four contemporary 100 sec dark frames. The brightness scale runs from 5000 to 9000 e-/pixel. The four amplifier locations are labeled A, B, C, and D.

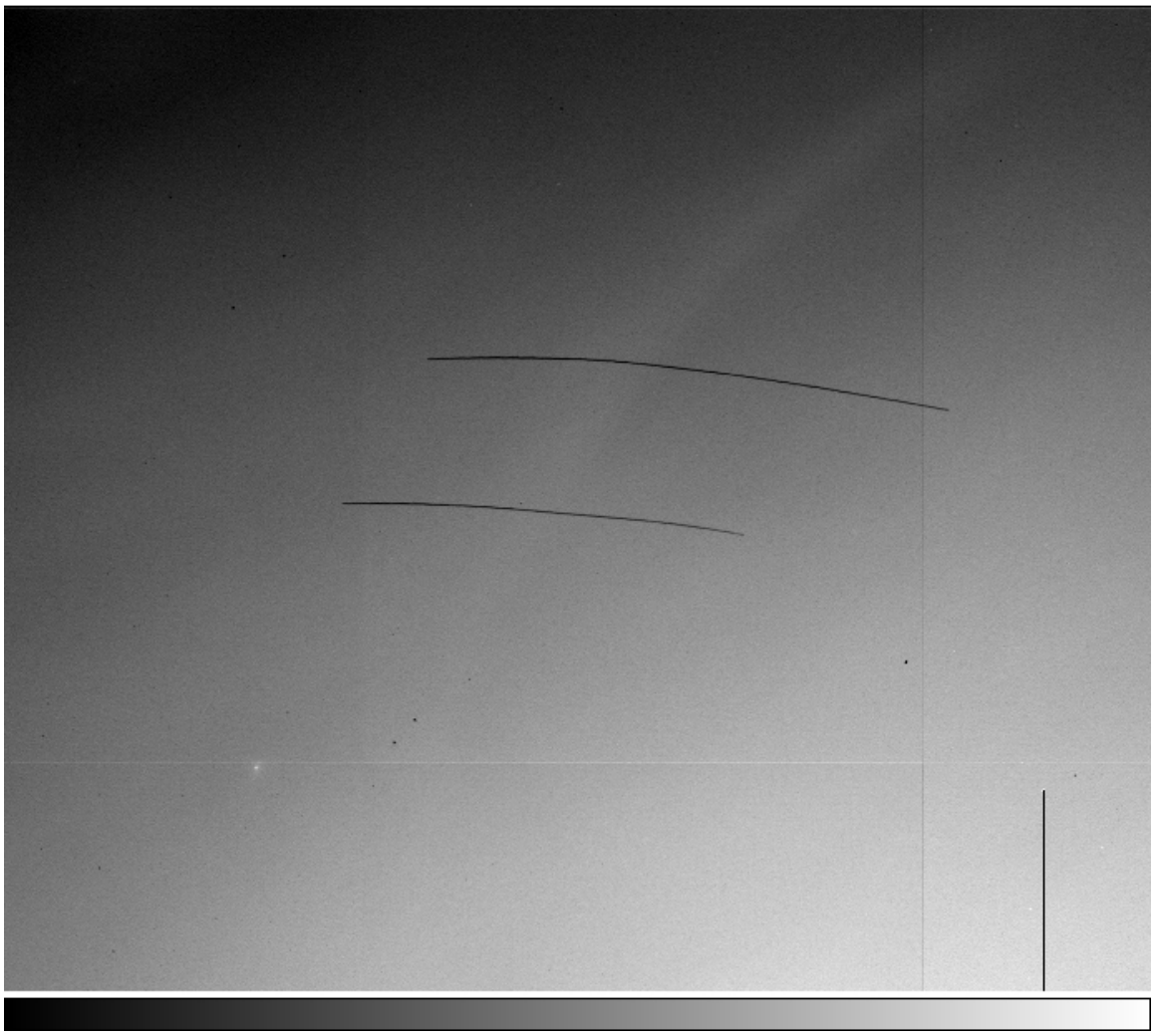

Figure 7. Detail of Figure 6 showing some of the features visible in a highly exposed flash image. The display is about 1400 pixels wide and centered near (x,y) = (2300, 3500); this region straddles the A and B amplifier quadrants. The brightness scale runs from 7000 to 9000 e-/pixel.

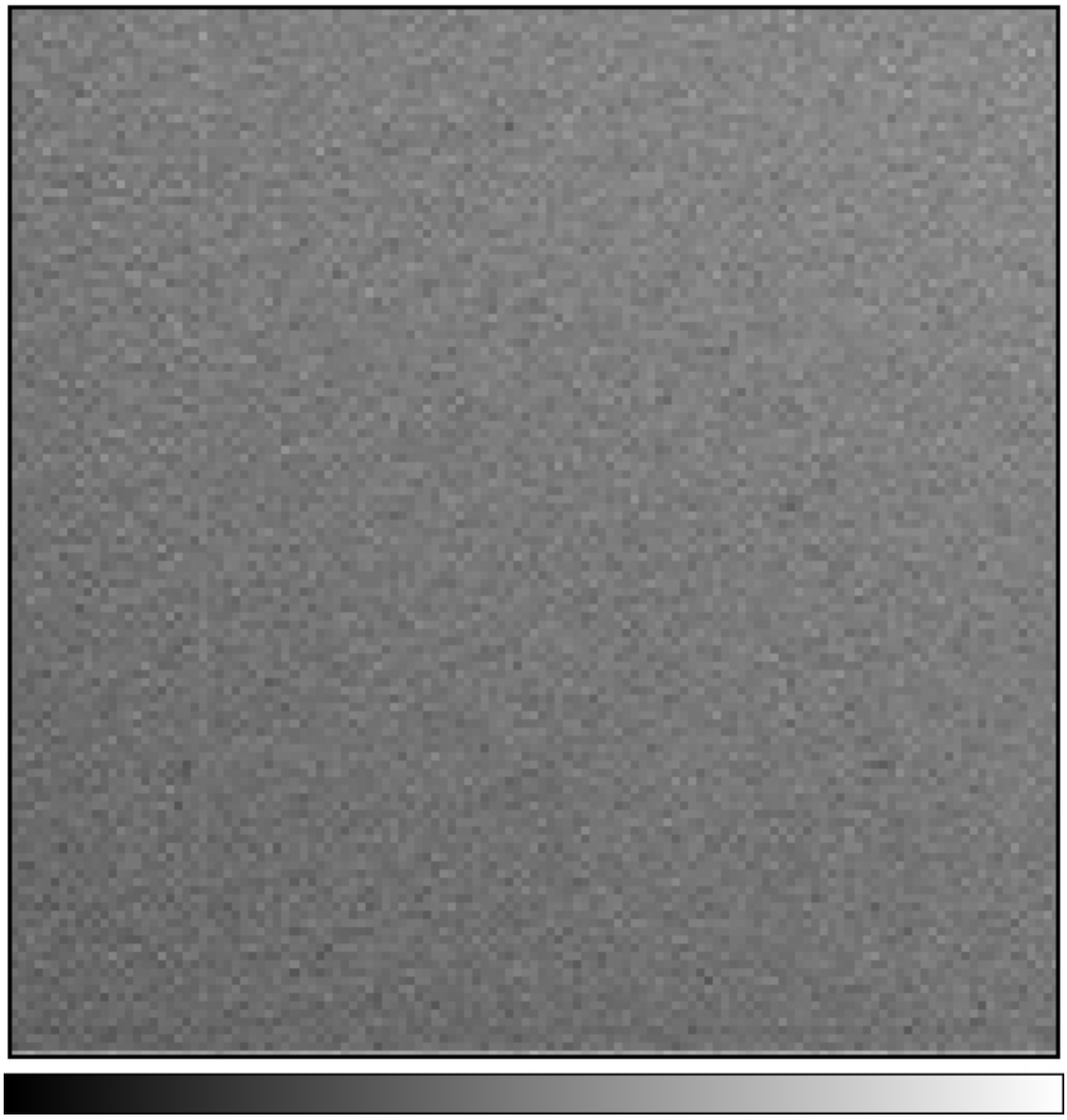

Figure 8. Detail of Figure 6 showing a 128 x 128 pixel region near the C amplifier. The brightness scale runs from 5000 to 7000 e-/pixel. The C amplifier is at the lower left. This is the same region as shown in Figure 5.

Both the A and B shutters can be used for the post-flash. While the shutters are similar, it is quite conceivable that small differences in their construction or finish (paint, etc.) could lead to differences in the resulting post-flash image. We examined this by taking four flash images with FLASHCUR=MED and FLASHDUR=100 made on each shutter, summing them with

cosmic ray rejection (using STSDAS CRREJ), and then taking the ratio of the results for shutter A with that of shutter B. The resulting ratio image is shown in Figure 9. The image is relatively flat – this is expected since the shutter is far from the focal plane, and any detector-dependent features should divide out. The primary feature is a smooth gradient from the A amplifier corner of the field to the D amplifier. The ratio image is highest near the A amplifier with a local mean value of 1.082, and lowest near the D amplifier with a local mean of 1.047. The average ratio of shutter A / shutter B across the entire field of view is 1.067.

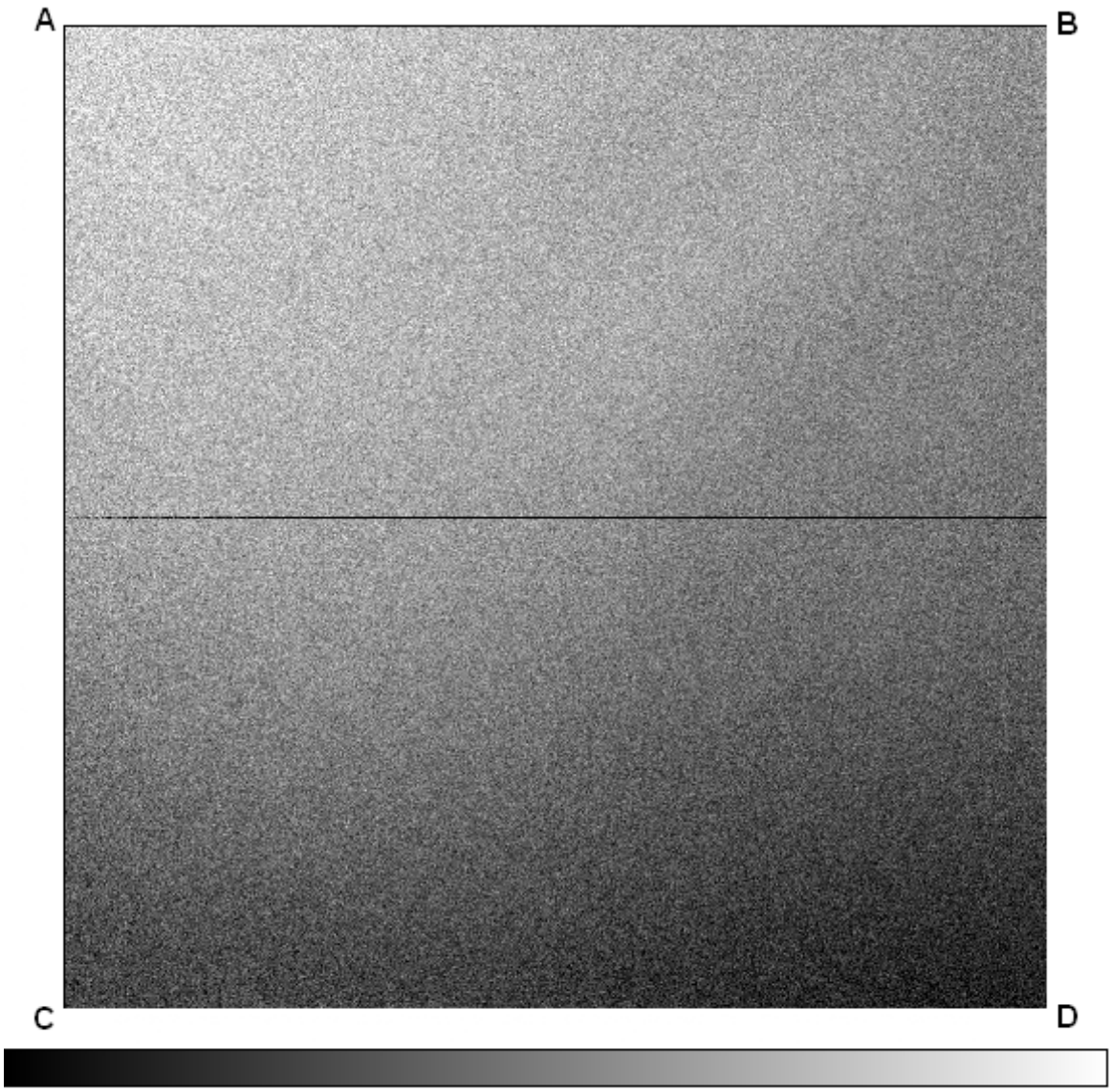

Figure 9. Ratio of shutter A / shutter B across the full field of view. The images are from proposal 13069 and are listed (among others) in Table 4 and Table 5. All images were taken back-to-back as pairs of shutter A and shutter B images, so as to minimize effects of brightness instability (discussed later). The brightness scale runs from 1.04 to 1.09. Locations of the four amplifiers are labeled A, B, C, and D.

We examined the short-term stability of the post-flash by computing the mean counts for 24 full-frame 0.5 sec darks flashed with FLASH=12 in shutter A from proposal 13069. This flash brightness is similar to that recommended to science observers. The images were taken between September 2 and October 18, 2012. The mean counts were computed over a 200x200 pixel region centered near the brightest part of the field near (x, y) = (2700, 2400). IRAF IMSTAT was used with 3 iterations of 3 sigma rejection to eliminate cosmic rays and

other artifacts. The average brightness among all the images was 15.38 e-/pixel with an RMS of 0.21 e-/pixel or 1.3% among the different images. The lowest value was 14.85 e-/pixel (3.4% below the mean) and the highest value was 15.72 e-/pixel (2.3% above the mean). The combined photon and read noise in the mean counts for these images is only about 0.16% [6], so the observed scatter is not due to simple noise. Apparently there is instability in the brightness of the post-flash at the ~1.3% RMS level on time-scales of 6 weeks or less. This instability should not significantly impact most science observations, as it is small compared to other sources of sky and background variations, and the post-flash light pattern is relatively flat. The instability is discussed further in a later section of this report.

We investigated the linearity of the post-flash LED lamp since there is some previous evidence for a non-linear relationship between flash duration and resulting counts per pixel. We measured the count rate as function of flash duration (FLASHDUR), and plot the result in Figure 10 for LOW current, shutter A, and the C1K1C sub-array.[7] From left to right the data points correspond to FLASH=3, 5, 8, 10, 12, and 20 e-/pixel. The final value on the right was obtained with FLASHEXP=100 and FLASHCUR=LOW. Only data from November 15 and 16, 2012 are used in an effort to minimize the impact of the previously noted instability in the flash brightness (as discussed later the instability appears to be reduced on shorter timescales). The count rate is highest for very short flash times with values ~2.62 e-/sec/pixel, and decreases monotonically with flash duration and reaches ~2.44 e-/sec/pixel at FLASHDUR=100. The C1K1C aperture was used for these observations since it has a short read-out time. It is in a relatively faint region of the post-flash light distribution, which should be kept in mind when comparing values mentioned here and elsewhere in this report.

The MEDIUM current setting shows a similar non-linearity and is illustrated in Figure 11. The data points from left to right represent FLASH=15 and 22 (FLASHDUR=0.2 and 0.3 sec), with the right-most point being FLASHDUR=100 sec.[8] The count rate decreases from ~73 e-/sec/pixel to ~67 e-/sec/pixel as the flash duration increases. For a given flash duration, the count rate for MEDIUM current is approximately 27 times brighter than the LOW current setting.

The non-linearities shown in Figure 10 and Figure 11 represent about 8% non-linearity

[6] Estimated as sqrt(readnoise^2 + e-)/sqrt(# pixels)/(e-) = sqrt(3x3 + 15.7)/sqrt(200x200)/15.7 = 0.16%.

[7] The data in Figure 10 are from program 13078 visits A3, A6, A7, and A8 and taken on November 15 and 16, 2012. Images were combined in pairs with STSDAS CRREJ, and the mean pixel value was computed for the 1024x1024 pixel area nearest the C amplifier using IMSTAT with 3 iterations of 3 sigma rejection.

[8] The data for Figure 11 are from program 13078 visits A3, A4, A5, and A6 taken on November 14 and 15, 2012. The images were analyzed in the same way as those in Figure 10.

between short and long flash durations. This is much larger than non-linearity seen in the detector (e.g. Gilliland, Rajan, and Deustua 2010), and hence must arise in the LED circuitry or commanding of its operation. The non-linearity should not directly affect most science data, since typically a single flash level (FLASHDUR) is used for similar images within an observation. But it could potentially affect the post-flash calibration when reference files obtained at one flash level are applied to science data taken with a different flash setting; this will need to be addressed when generating the reference files.

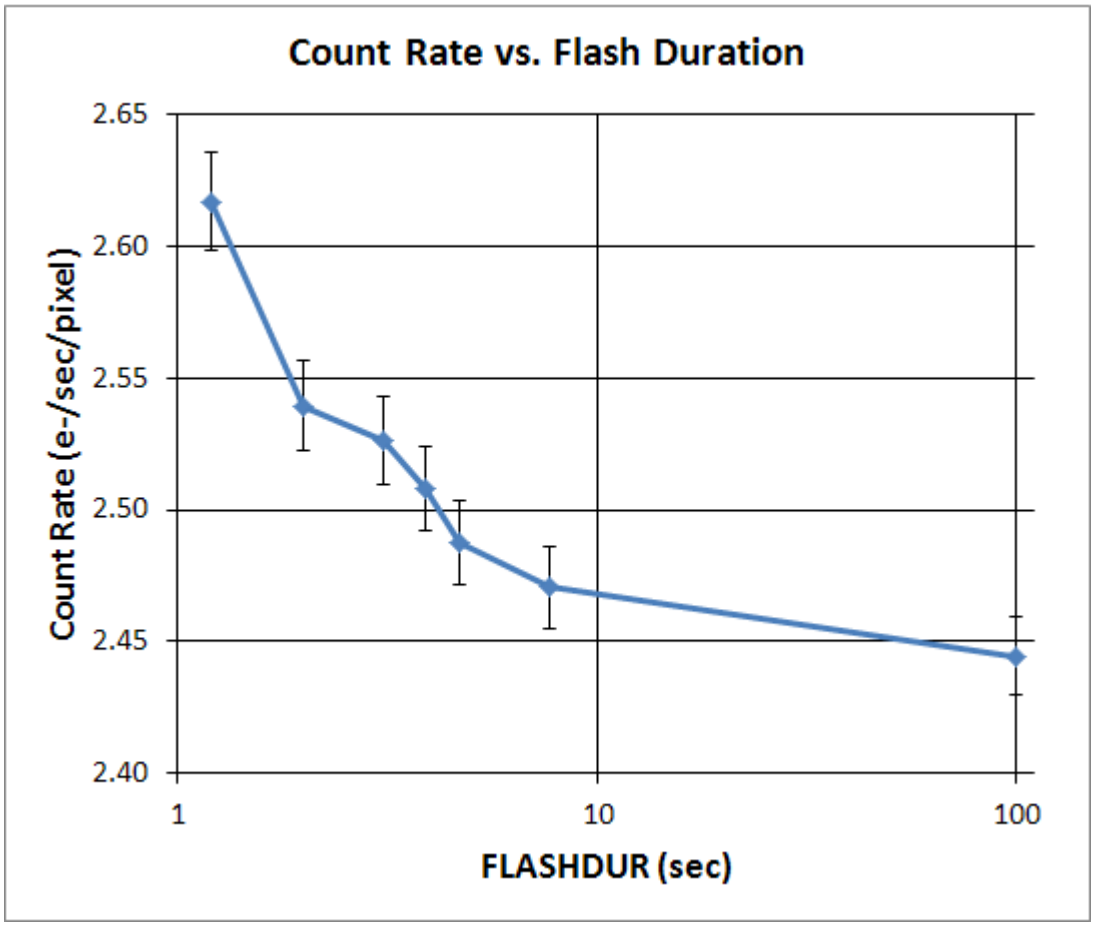

Figure 10. Count rate in e-/sec/pixel as a function of flash duration (FLASHDUR in sec) for LOW current and shutter A in the C1K1C sub-array. The uncertainties are estimated at ~0.6% from the post-flash instability on 1-day timescales.

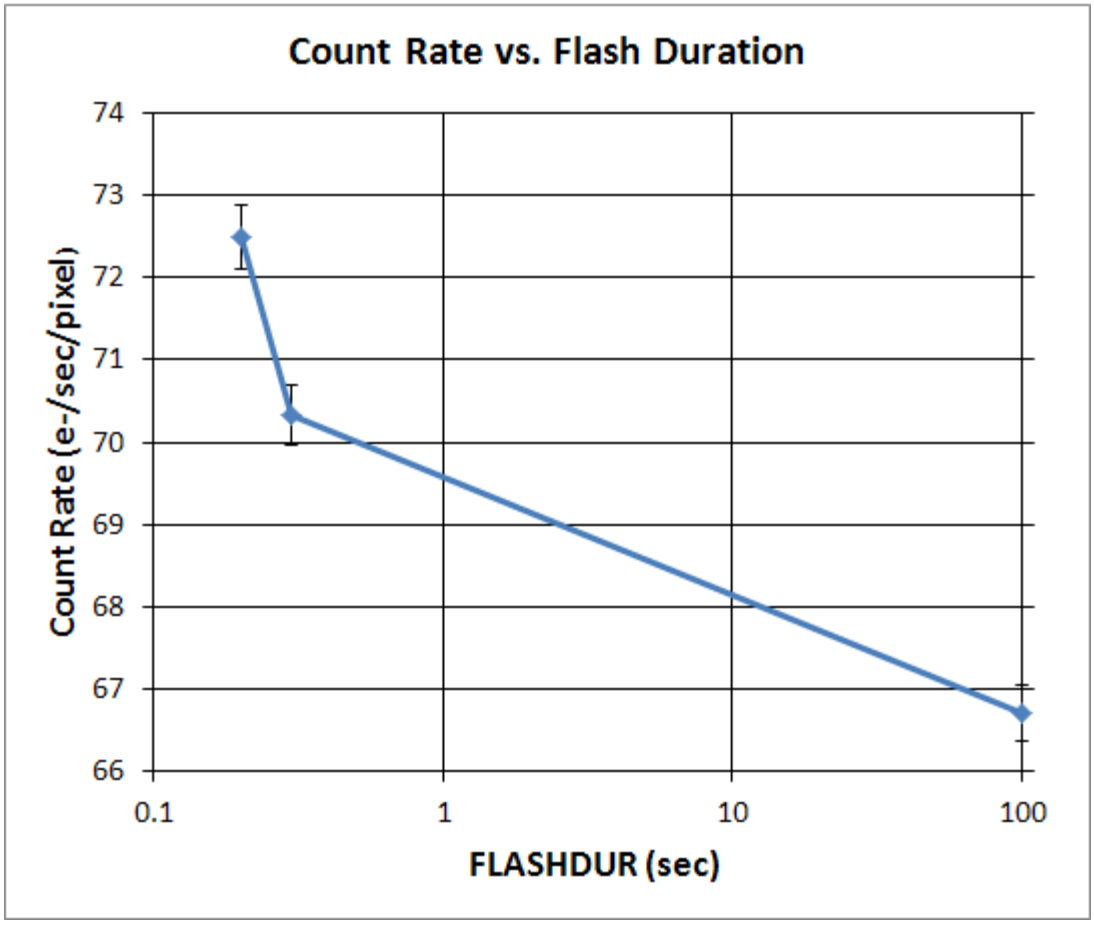

Figure 11. Count rate in e-/sec/pixel as a function of flash duration (FLASHDUR in sec) for MEDIUM current and shutter A in the C1K1C sub-array. The uncertainties are dominated by instabilities in the flash brightness of ~0.5%.

Calibration of Science Data: CALWF3 and the Calibration Pipeline

Science data are automatically calibrated by the calibration pipeline using the CALWF3 software. This process is controlled by a number of data header parameters in the raw image files. The header parameters related to post-flash calibration are listed in Table 3. SHUTRPOS, BINAXISx, and DATE-OBS are not specific to post-flash calibration, but are used by the pipeline when selecting the appropriate post-flash reference file.

We performed various tests on CALWF3 in an attempt to understand and verify its handling of post-flashed data. CALWF3 uses the post-flash reference file listed in the FLSHFILE parameter, multiplies this file by the lamp on-time (FLASHDUR), divides by a gain value, and then subtracts the post-flash image from the science image. Hence the required reference file

is in units of e-/pixel per second of lamp on-time. These steps are performed after bias calibration, but before cosmic ray rejection, dark subtraction, and flat field calibration (c.f. WFC3 Data Handbook).

The FLSHFILE value is populated by the calibration pipeline prior to processing. The best reference file is selected based on the values of FLASHCUR, SHUTRPOS, and DATE-OBS.

The gain value used by CALWF3 during post-flash calibration requires some discussion. Our tests indicate it uses a gain value of 1.56 for all four amplifiers, for the default nominal value of GAIN=1.5 in the phase II proposal. From the WFC3 Instrument Handbook and the CCD reference file, this appears to be the exact value only for amplifier C. It is also the value populated in all four header values of ATODGNA, ATODGNB, ATODGNC, and ATODGND by CALWF3.[9] It appears that CALWF3 uses the gain value for amplifier C from the CCD reference file for all four amplifiers when performing post-flash calibration. We will need to use this same value when constructing the reference file, so as to ensure proper scaling and subtraction of the post-flash.

The pixel format of the post-flash reference file has been a source of some confusion. On-line documentation of the calibration reference file formats indicated it had a format similar to the flat field reference files (6 groups of 4096x2051 pixels), while other documentation indicated a format more similar to the bias reference files which include over-scan regions (6 groups with 4206x2070 pixels). We performed tests on CALWF3 using both formats. The latter 4206x2070 pixel format gave correct results, while the former 4096x2051 format did not. Hence we have assumed the correct format for the post-flash reference file to be the 4206x2070 pixels format similar to the bias reference file.

[9] A decision was made when designing CALWF3 to use a single gain value for all four amplifiers, and then let the flat field reference file handle the gain differences between the amplifiers. Apparently this philosphy for the flat-field calibration was carried over to the post-flash calibration.

Table 3. Data header parameters related to post-flash calibration.

Header Parameter	Definition	Value Range	Units
FLASHDUR	Post-flash lamp on-time	0.1 to 409.5	sec
FLASHCUR	Post-flash current setting	ZERO, LOW, MED, HIGH	
FLASHLVL	Requested flash level (phase II FLASH value)	0 to 25	e-/pixel
FLASHSTA	Status of the post-flash exposure	SUCCESSFUL, ABORTED, NOT PERFORMED	
FLSHCORR	Calibration control switch and status of post-flash calibration	PERFORM, OMIT, COMPLETE	
FLSHFILE	Post-flash calibration reference file name		
MEANFLSH	Computed mean counts in the post-flash reference file after multiplying by FLASHDUR and dividing by the gain. Includes over-scan regions.		counts/pixel
SHUTRPOS	Position of the shutter at the end of the exposure	A, B	
BINAXIS1, BINAXIS2	On-chip binning mode	1, 2, 3	
DATE-OBS	Observation date		
ATODGNA, ATODGNB, ATODGNC, ATODGND	Gain value assumed by CALWF3 during calibration		e-/count

Calibration Reference Files: LOW Current with Un-binned Pixels

The vast majority of observer post-flash utilization involves the LOW current setting (Figure 1, Table 1) with un-binned pixels, hence our first priority was to generate the reference files for LOW current. The strategy was to use highly exposed post-flash images taken with the MEDIUM current setting and 100 sec lamp on-time, correct these for dark current, and then scale them to the appropriate level for a LOW current reference file. Since no post-flashed dark current reference files would be available at this point in time, the data would be dark

calibrated outside the usual CALWF3 pipeline. Due to expected differences in the shutter reflectivities, separate reference files are made for the A and B shutters.

The A shutter image was generated as follows, using images flashed with shutter A. The raw images used are summarized in Table 4. First a high signal-to-noise ratio MEDIUM current flash image was generated using four 100 sec flash images from proposal 13069: ic3mc0dtq, ic3mc2e2q, ic3mc4e4q, and ic3mc6ebq. The images were recalibrated in CALWF3 applying only bias level and bias image calibrations. They were then combined using the STSDAS CRREJ task with appropriate noise and gain settings for WFC3. The combined image contained approximately 31000 e-/pixel, and hence will have an RMS noise level of about 0.6% per pixel.

This image was corrected for dark current using four 100 sec dark frames also from program 13069 and observed on the same day as the flash images: ic3mc1erq, ic3mc3f1q, ic3mc5eyq, and ic3mc7fcq. These darks were obtained with a 0.3 sec MEDIUM current flash (i.e. FLASH=22) to minimize CTE losses on warm and hot pixels. These were also re-calibrated in CALWF3 and combined in the same way as the flash images. The resulting dark image was then subtracted from the flash image, yielding a dark-corrected MEDIUM current flash image. This image was then divided by four (since CRREJ sums). The net result was an image with an effective flash duration of (100 – 0.3) = 99.7 sec and a residual dark time of (100.5 – 100.3) = 0.2 sec. [10]

Next we needed to derive a scaling factor to convert this image to the appropriate level for a LOW current image with an effective 1 sec lamp on-time. Since the total flash counts are known to be slightly non-linear with flash duration (see previous discussion herein), we used a typical FLASH=12 (12 e-/pixel LOW current) flash to perform the scaling. This is similar to the flash level recommended to observers, and hence should minimize the impact of non-linearity. Four 12 e-/pixel LOW current flash images (4.7 sec flash duration) were used, also from program 13069 and observed within a few days of the other images: ic3md0y7q, ic3md1zvq, ic3md2opq, and ic3md3stq. The default pipeline calibrated images were used, and were combined with CRREJ. The normal dark calibration was not very good when applied to these flashed images, but is probably adequate for our purposes since the exposure is short and we only require an average brightness (i.e. poorly corrected hot pixels can be statistically rejected).

[10] The 100 sec flash images are commanded as 0.5 sec dark frames, and hence have a total dark time of 100.5 sec. The 100 sec dark frames have FLASH=22 and hence have a total dark time of 100.3 sec. An iterative solution for the dark calibration is not needed, since the dark times of the 100 sec dark frames and the bright FLASHDUR=100 flash images are nearly equal.

The effective flash in 1 sec was computed for both the MEDIUM and LOW current images by dividing by the appropriate flash durations (i.e. 99.7 sec [11] and 4.7 sec, respectively), and finally the ratio image of the LOW / MEDIUM current was computed. IRAF task IMSTAT was used to compute the average ratio of LOW / MEDIUM current brightness across the image using 3 cycles of 2 sigma rejection (USIGMA=LSIGMA=2). The resulting brightness ratio between LOW and MEDIUM current was 0.03654. For making reference files we used the average value for shutters A and B of 0.03639, since the ratio should be independent of shutter, and this would reduce the effects of noise.

The high signal-to-noise MEDIUM current flash image was then scaled to produce the LOW current reference file. It was divided by 99.7 sec, and multiplied by 0.03639 to convert it to an effective LOW current 1 sec image. Finally it was multiplied by 1.56 to convert it to e-/pixel. The periphery of each image quadrant was then padded with zeros to provide the correct 4206x2070 pixel format needed by CALWF3. The noise array and data quality bits (groups [2],[3],[5], and [6]) were set to zero. The image was delivered to CDBS on November 29, 2012 and named wc52031oi_fls.fits. The reference file is shown in Figure 12.

The shutter B reference file was produced in much the same way, but using images that had been flashed on shutter B (Table 5). For the MEDIUM current 100 sec flash images we used ic3mc0dwq, ic3mc2e0q, ic3mc4e6q, and ic3mc6e8q. For the 100 sec dark frames we used ic3mc1etq, ic3mc3f3q, ic3mc5ewq, and ic3mc7f9q. And finally, the four LOW current images used to scale the MEDIUM current image were ic3md0y9q, ic3md1ztq, ic3md2owq, and ic3md3swq. The brightness ratio between LOW and MEDIUM current for shutter B was 0.03623. This image was also delivered to CDBS on November 29, 2012 and was named wc52031pi_fls.fits. The shutter B reference file is shown in Figure 13; it is very similar to the shutter A reference file, but has ~7% lower values, and a ~4% gradient running from amplifier A to amplifier D (e.g. Figure 9).

Both reference files were extensively tested prior to delivery. They were applied to several science images, and accurate subtraction of the post-flash was verified. We were also concerned about the format of the reference file, and proper padding of the image periphery, so the registration of the reference files were checked against the science images. The location of bright hot pixels in each detector quadrant were measured in both the reference file, and the raw and calibrated science images, and found to be in agreement.

[11] The effective flash duration for the FLASHCUR=MED, FLASHDUR=100 sec bright flash is reduced by 0.3 sec, since the 100 sec dark frame (which was subtracted for dark calibration) contained a 0.3 sec flash. This calculation is not perfect due to non-linearities, but the net error is extremely small.

Table 4. Ingredients for the LOW current, un-binned reference file for shutter A.

Image Name	Image Type	FLASHCUR	FLASHDUR	EXPTIME	SHUTRPOS	DATE-OBS
ic3mc0dtq ic3mc2e2q ic3mc4e4q ic3mc6ebq	DARK	MED	100 sec	0.5 sec	A	2012-10-15
ic3mc1erq ic3mc3f1q ic3mc5eyq ic3mc7fcq	DARK	MED	0.3 sec	100 sec	A	2012-10-15
ic3md0y7q ic3md1zvq ic3md2opq ic3md3stq	DARK	LOW	4.7 sec	0.5 sec	A	2012-10-17 to 2012-10-18

Table 5. Ingredients for the LOW current, un-binned reference file for shutter B.

Image Name	Image Type	FLASHCUR	FLASHDUR	EXPTIME	SHUTRPOS	DATE-OBS
ic3mc0dwq ic3mc2e0q ic3mc4e6q ic3mc6e8q	DARK	MED	100 sec	0.5 sec	B	2012-10-15
ic3mc1etq ic3mc3f3q ic3mc5ewq ic3mc7f9q	DARK	MED	0.3 sec	100 sec	B	2012-10-15
ic3md0y9q ic3md1ztq ic3md2owq ic3md3swq	DARK	LOW	4.7 sec	0.5 sec	B	2012-10-17 to 2012-10-18

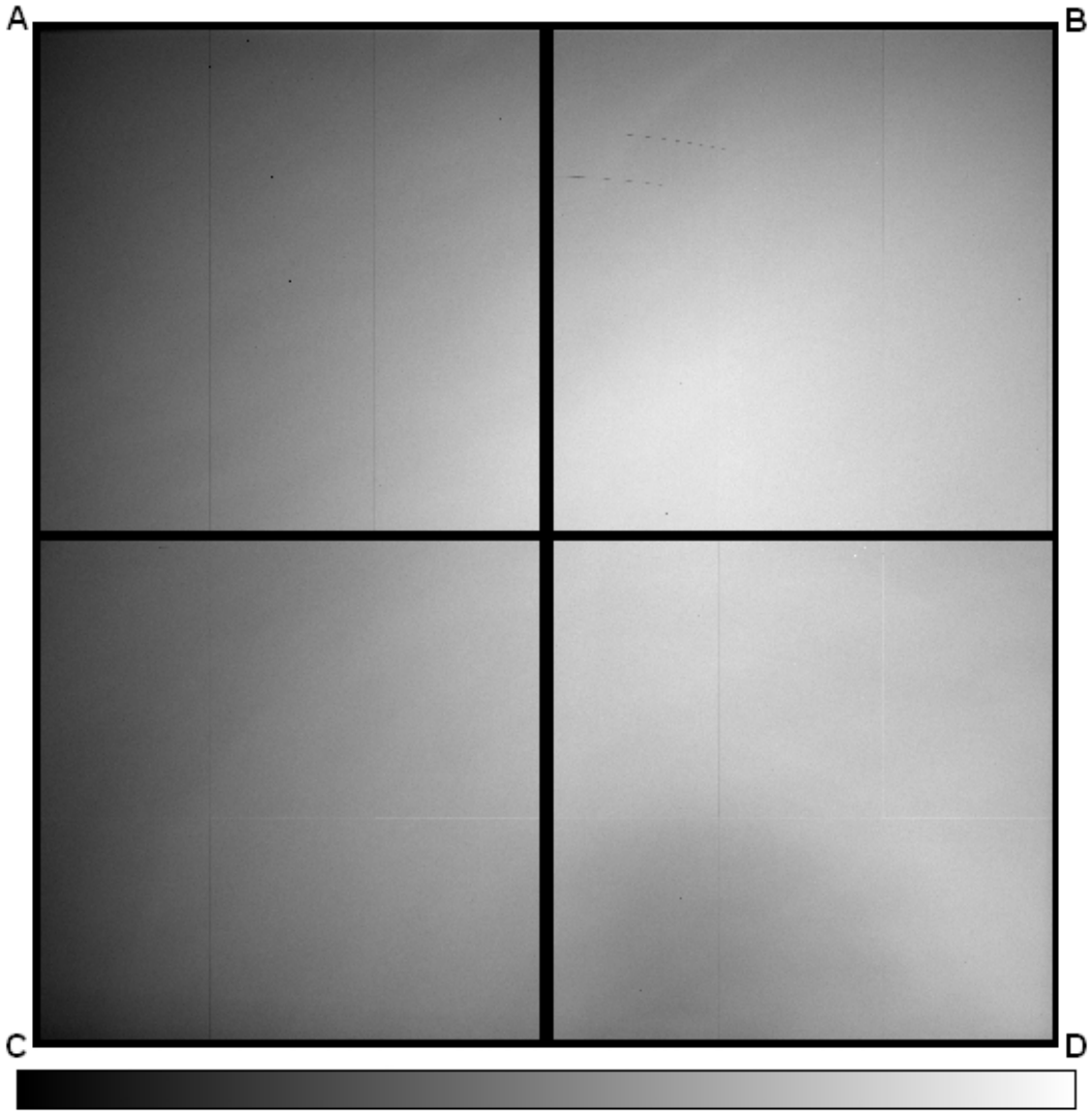

Figure 12. Post-flash reference file wc52031oi_fls.fits for LOW current and shutter A. The dark borders are over-scan regions which are required by CALWF3. The brightness scale runs from 2.0 to 3.4 e-/sec/pixel. Locations of the amplifiers are labeled A, B, C, and D.

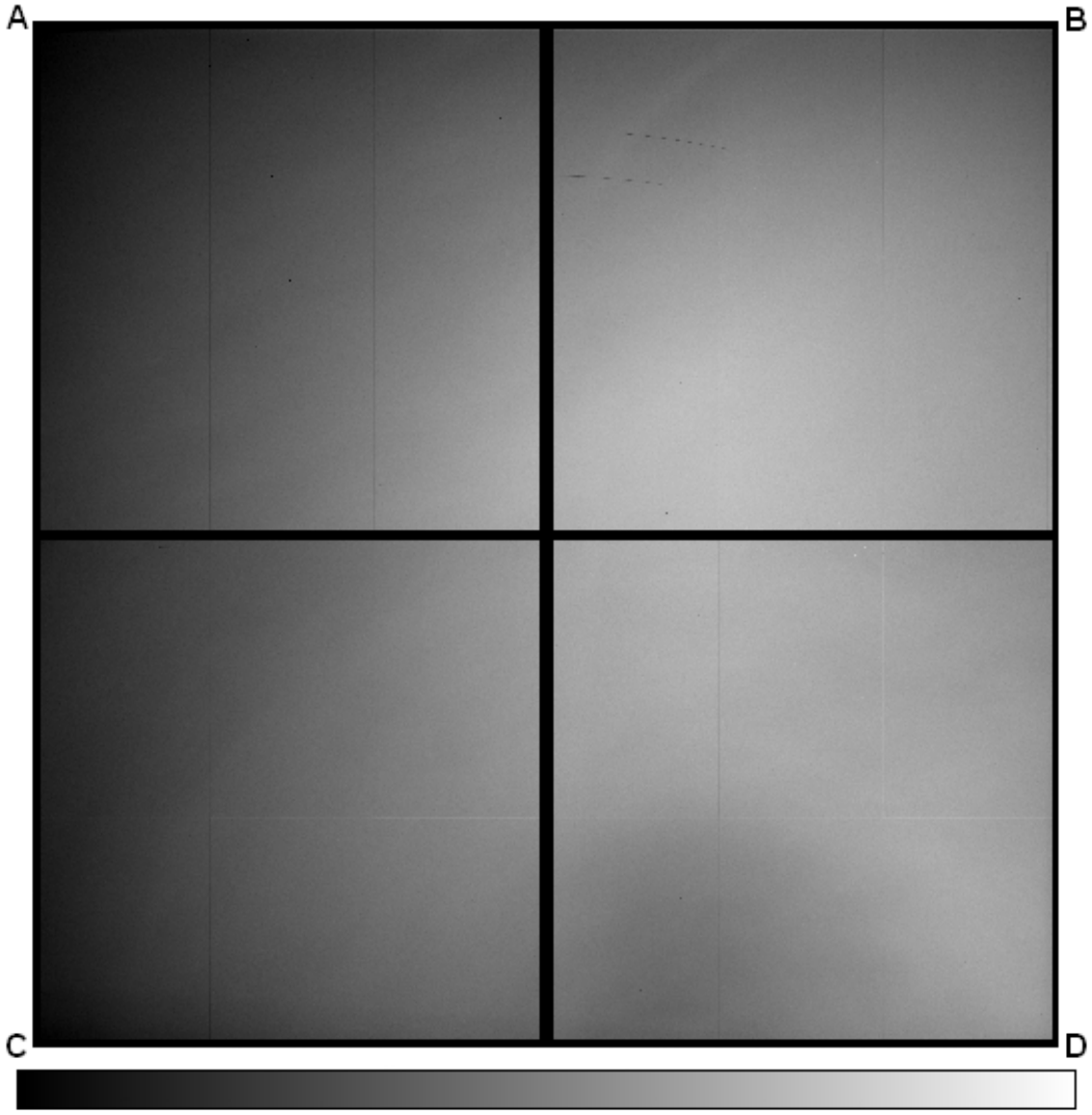

Figure 13. Post-flash reference file wc52031pi_fls.fits for LOW current and shutter B. The dark borders are over-scan regions which are required by CALWF3. The brightness scale runs from 2.0 to 3.4 e-/sec/pixel. Locations of the amplifiers are labeled A, B, C, and D.

Calibration Reference Files: MEDIUM Current with Un-binned Pixels

Science observations using the MEDIUM flash current setting were planned for mid-April 2013. Reference files for this mode were created as follows. The strategy would be to simply re-scale the existing LOW current reference files, so as to make them appropriate for

MEDIUM current. First we established the observed brightness ratio between the MEDIUM and LOW current settings. Since the total flash counts are known to be non-linear with lamp time, we selected images with FLASH values similar to those expected for typical science observations. We used six images each with FLASH=15 e-/pixel (MEDIUM current) and FLASH=12 e-/pixel (LOW current) taken with the C1K1C sub-array. The images are from proposal 13078 are listed in Table 6 and Table 7. The images were selected in LOW current / MEDIUM current pairs that were taken close in time, so as to minimize the effects of the brightness instabilities previously noted.

Pipeline calibrated images were used. Each group of 6 images was combined with cosmic ray rejection using the STSDAS task CRREJ, with appropriate settings for WFC3. For each shutter the ratio image of FLASH 15 / FLASH 12 was computed, and the mean value over the ratio image was computed using IMSTAT with limits 1.0 to 1.5, which span the expected ratio ~1.25. The resulting ratios were shutter A: 1.233, and shutter B: 1.232.

The above exposures were made using flash times of 0.2 sec for MEDIUM current, and 4.7 sec for LOW current. Hence the brightness ratio in counts per second between the MEDIUM and LOW current settings is (averaging results for the two shutters):

1.2325 * 4.7 / 0.2 = 28.96

Finally the reference files for LOW current were multiplied by this scaling factor and re-delivered as reference files for MEDIUM current. The LOW current reference files used were: shutter A: wc52031oi_fls.fits, and shutter B: wc52031pi_fls.fits. The delivered MEDIUM current files were x45f1554li_fls.fits and x45f1554mi _fls.fits for shutters A and B, respectively, and were delivered on April 15, 2013. We have not displayed the MEDIUM current reference files as they are indistinguishable from the LOW current referenced files, other than an overall scaling factor.

The reference files for both LOW and MEDIUM current are summarized in Table 8.

Table 6. Ingredients for the MEDIUM current, un-binned reference file for shutter A.

Image Name	Image Type	FLASH	FLASHCUR	FLASHDUR	EXPTIME	SHUTRPOS	DATE-OBS
ic6da3uqq ic6da6wuq ic6db3slq ic6dc3jkq ic6dd3y8q ic6de3rqq	DARK	15	MED	0.2 sec	0.5 sec	A	2012-11-15 2012-11-15 2012-12-16 2013-01-12 2013-02-09 2013-03-09
ic6da2c7q ic6da5qpq ic6db2t1q ic6dc2k4q ic6dd2ydq ic6de2u5q	DARK	12	LOW	4.7 sec	0.5 sec	A	2012-11-16 2012-11-14 2012-12-16 2013-01-12 2013-02-09 2013-03-09
wc52031oi_fls						A	

Table 7. Ingredients for the MEDIUM current, un-binned reference file for shutter B.

Image Name	Image Type	FLASH	FLASHCUR	FLASHDUR	EXPTIME	SHUTRPOS	DATE-OBS
ic6da3uiq ic6da6x2q ic6db3sdq ic6dc3jsq ic6dd3y0q ic6de3rgq	DARK	15	MED	0.2 sec	0.5 sec	B	2012-11-15 2012-11-15 2012-12-16 2013-01-12 2013-02-09 2013-03-09
ic6da2c3q ic6da5qtq ic6db2t5q ic6dc2k8q ic6dd2yhq ic6de2u9q	DARK	12	LOW	4.7 sec	0.5 sec	B	2012-11-16 2012-11-14 2012-12-16 2013-01-12 2013-02-09 2013-03-09
wc52031pi_fls						B	

Table 8. Summary of delivered reference files.

Reference File Name	FLASHCUR	SHUTRPOS	Delivery Date
wc52031oi_fls	LOW	A	2012-11-29
wc52031pi_fls	LOW	B	2012-11-29
x45f1554li_fls	MED	A	2013-04-15
x45f1554mi_fls	MED	B	2013-04-15

Calibration Reference Files for Other Modes

There are a total of 18 reference files needed to fully calibrate all potential implementations of the post-flash capability. This encompasses three current levels, three binning modes, and two shutter positions. At this point we have only delivered four of the 18 files. So far there are no user modes which utilize the HIGH current setting, and given that its count rate is only slightly higher than the MEDIUM setting, it is not clear it would ever be used. Post-flashed 2x2 binning mode has only been used by one program, where observers wanted to make their own reference files.[12] Nonetheless, we should provide reference files for this mode so that future archival users will have full calibration. Work on these reference files is underway, and preliminary versions have been generated, but testing is more complex and has not yet completed. Post-flashed 3x3 binning mode has not been used by any observers, and we have no immediate plans to deliver reference files for it. It may be efficient to wait and deliver reference files when they are needed, as the post-flash calibration is not yet mature and unexpected issues may appear.

Long-term and Short-term Stability

The long-term stability is of some concern as the LED lamp used for the post-flash may become dimmer with usage and age. This could ultimately impact the longevity of the reference files. Figure 14 shows the long-term behavior for 0.5 sec full-frame darks with FLASH=12; these images are comparable to what observers with very low background filters / targets might experience. The mean brightness in a 200x200 pixel region near the brightest part of the field is plotted. IRAF IMSTAT was used with 3 iterations of 3-sigma rejection to remove cosmic rays and other artifacts. The data show obvious, quasi-random variations with an RMS of 1.2% in shutter A and 1.0% in shutter B. Figure 14 also shows some correlation of the shutter A and B values, which are typically taken a few minutes apart on the same orbit; hence the stability must be better on orbit timescales. As expected, shutter A is about 7% brighter than shutter B.

We also examined the stability on one-day timescales. Figure 15 shows a few days of heavily

[12] It is unlikely that there would ever be many science images in this mode since the primary motivation of binning is to reduce CCD readnoise in situations with very low background where the readnoise dominates the signal-to-noise ratio. For post-flashed images the photon noise of the flash dominates, so that binning has very little benefit.

sampled data for FLASH=12 in the B shutter. The data on any given day are more tightly grouped, and there is a gradual drift over the 7 days. Using these data, and other data for both shutters we find that the RMS fluctuation on 1-day timescales is ~0.6%.

Figure 16 shows similar results for much brighter flashes (FLASHCUR=MED, FLASHDUR=100 sec) that are used to derive the reference files. Again the mean values for a 200x200 pixel region near the brightest part of the field are plotted. The data here also show quasi-random variations, though the RMS is lower, being 0.5% for both shutters. There are at least two data points taken on different orbits at each epoch for each shutter – in many cases the points overlap and appear as a single point in the plot. Apparently the brightness can be highly stable on timescales of hours, though is not always so.

In summary, we do not see any evidence of long-term dimming of the LED lamp at this point in time. Instead the long-term trending appears to be dominated by quasi-random fluctuations with an RMS ~1.2%. Shutter A and B data taken on the same orbits are correlated, and the RMS on 1-day timescales is ~0.6%, which indicates better stability on short timescales.

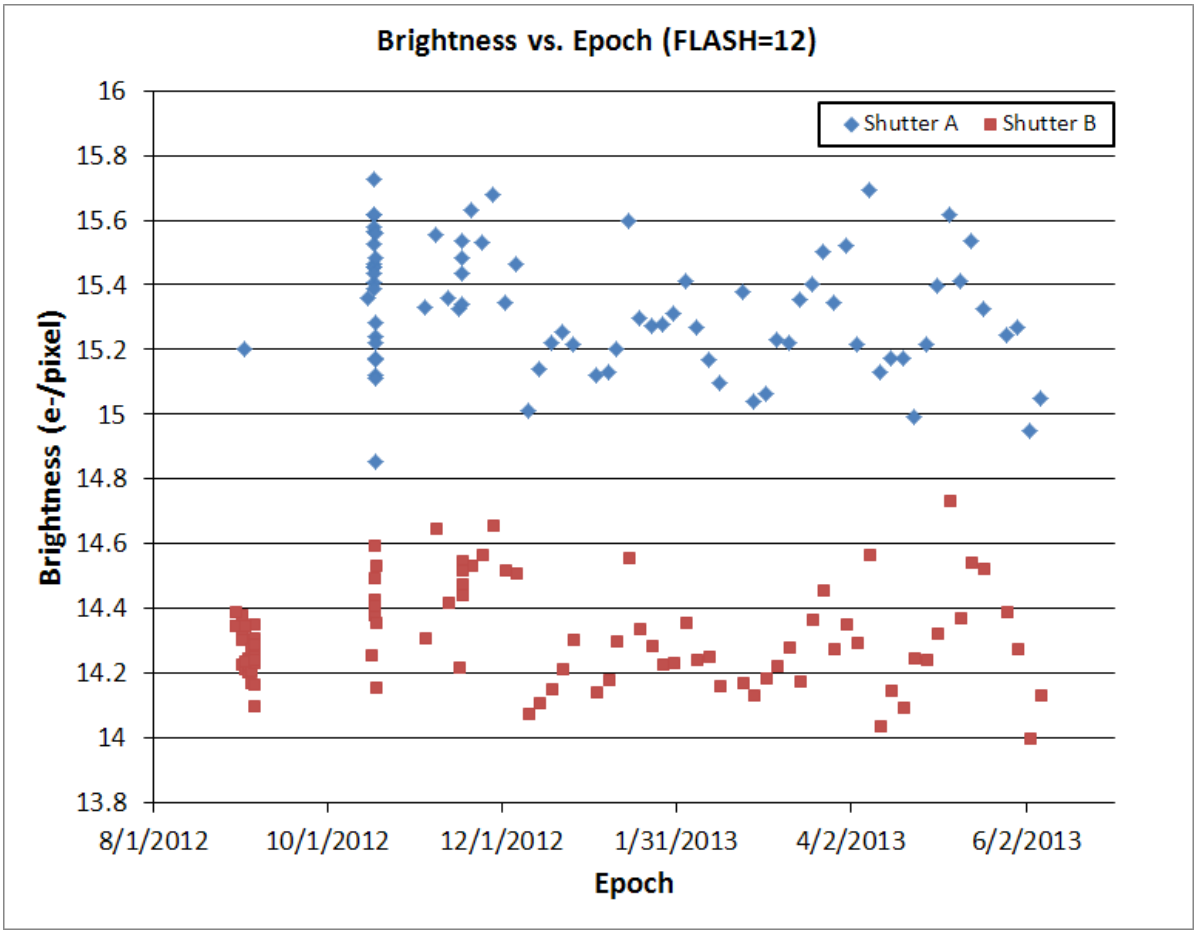

Figure 14. Brightness vs. epoch for full-frame 0.5 sec darks with FLASH=12. The mean brightness in a 200x200 pixel region near the brightest region of the field (x, y) = (2700, 2400) is plotted. The RMS is 0.19 and 0.15 e-/pixel for shutters A and B respectively. Uncertainties from combined read and photon noise are ~0.02 e-/pixel. Data are from proposals 13069, 13073, 13074, 13075, and 13078.

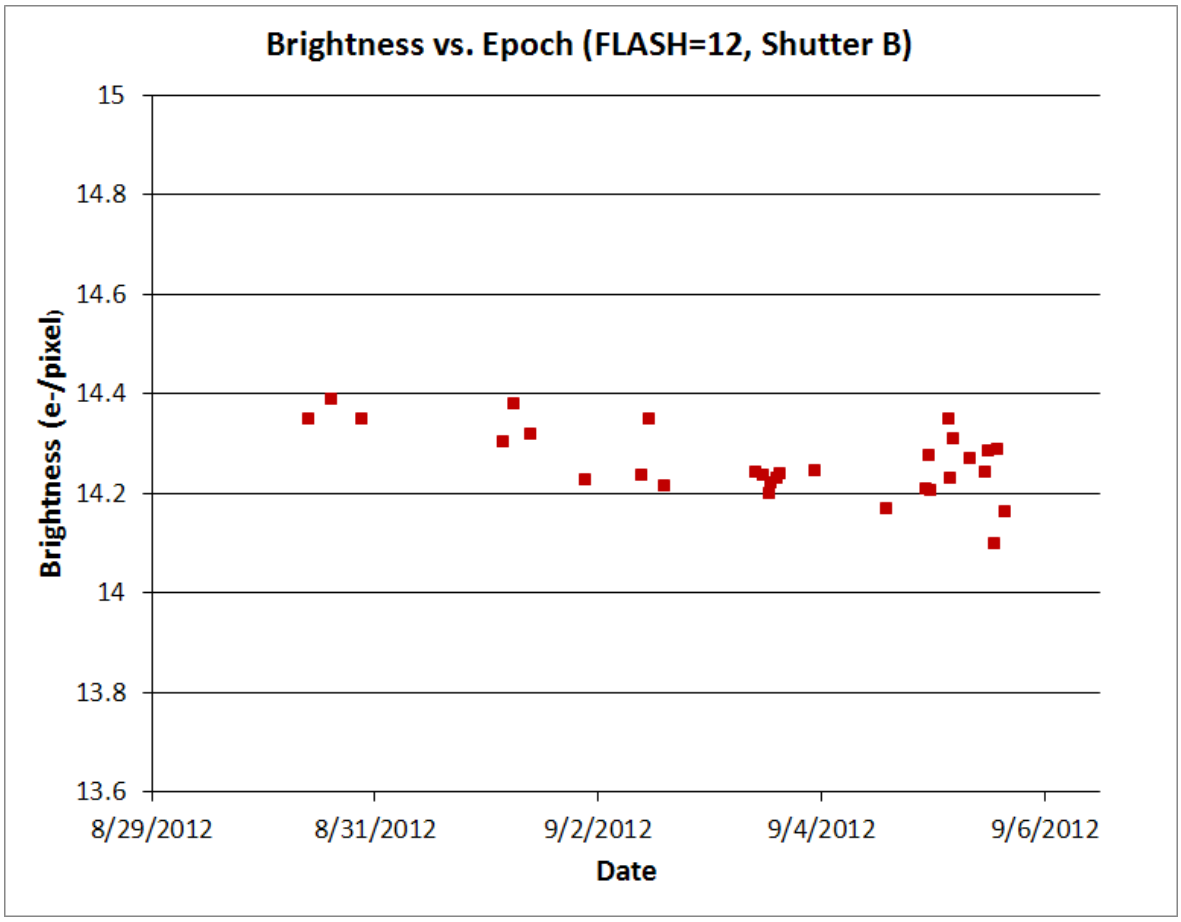

Figure 15. Brightness vs. epoch for full-frame 0.5 sec darks with FLASH=12. The mean brightness in a 200x200 pixel region near the brightest region of the field (x, y) = (2700, 2400) is plotted. From these and other data for both shutters, the RMS variation over a 1 day period is ~0.6%. Uncertainties from combined read and photon noise are ~0.02 e-/pixel. Data are from proposal 13069.

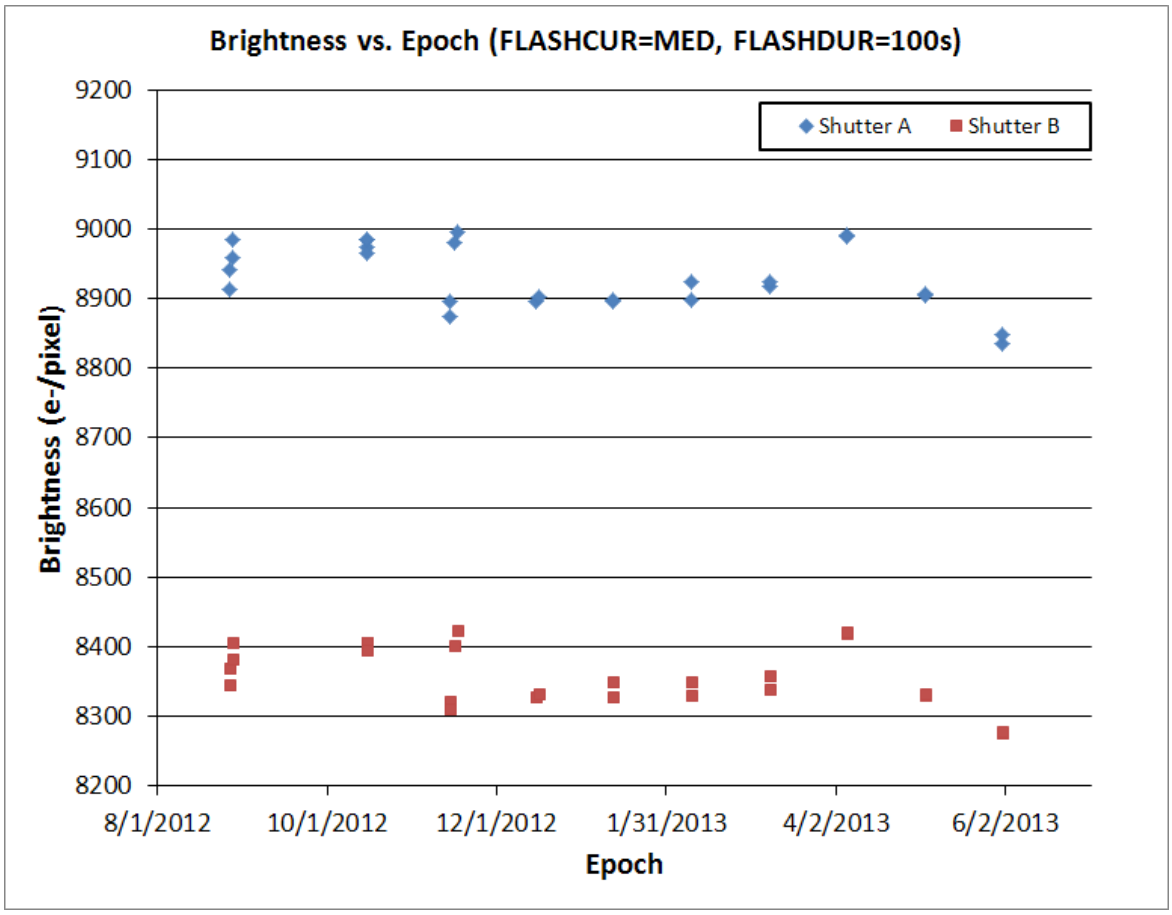

Figure 16. Brightness vs. epoch for full-frame 0.5 sec darks with FLASHCUR=MED and FLASHDUR=100 sec. The mean brightness in a 200x200 pixel region near the brightest region of the field (x, y) = (2700, 2400) is plotted. Many of the plotted points overlap – there are at least two points plotted for each shutter at each epoch. Uncertainties from combined read and photon noise are ~0.5 e-/pixel. The data are from proposals 13069 and 13078.

We tested for long-term changes in the illumination pattern of the post-flash as follows. We combined four FLASHCUR=MED, FLASHDUR=100 shutter A images with normal pipeline calibration from August 27-28, 2012 (ic3mb0eoq, ic3mb1fgq, ic3mb2h2q, and ic3mb3jfq) using STSDAS CRREJ, and compared the result to four similarly processed images from April – May, 2013 (ic6df1hnq, ic6df2jiq, ic6dg1m3q, and ic6dg2lmq). The difference image was computed and smoothed with a sigma=10 pixel Gaussian function to reduce noise. No changes were seen on these spatial scales exceeding ~0.1% in brightness. A few hundred scattered single pixels were seen to change at the 5% to 10% level, but we attribute these to variable hot pixels and other detector issues, and not to the post-flash calibration itself. Hence there appear to be no significant changes in the post-flash illumination pattern over a 7 month period at the ~0.1% level.

Concerns and Future Improvements

The post-flash reference files have several potential problems areas that have not yet been fully studied, as well as several known areas needing improvement.

We have assumed that the light distributions across the detectors of the LOW and MEDIUM lamp current settings are identical, and can be simply related by an overall scaling factor. This seems likely to be true, especially since a single LED is used for the post-flash, and the emissive area is very small compared to other relevant camera dimensions. But at some point the assumption should be verified.

The non-linearity in the post-flash brightness (i.e. Figure 10 and Figure 11) will result in small errors in the post-flash calibration, especially for flashes that are significantly brighter or fainter than the FLASH~12 level where the reference files were optimized. For example, the brightness scale of the LOW lamp current reference was established using FLASH=12 images (FLASHDUR=4.7 sec). If an observer uses FLASH=25 (FLASHDUR=9.7 sec) we can see from Figure 10 that the lamp count rate will be about 0.02 e-/sec/pixel lower than FLASH=12, or about 0.02 * 9.7 = 0.19 e-/pixel fainter than computed from the reference file. Hence the post-flash calibration will over-subtract the background by about 0.2 e-/pixel. For most observations this error will be unimportant. Similarly the MEDIUM current reference file was optimized for FLASH=15 (FLASHDUR=0.2 sec). From Figure 11 we can estimate that a FLASH=22 image will have the post-flash over-subtracted by about 2 e-/sec/pixel * 0.3 sec = 0.6 e-/pixel. Again this will probably be unimportant for most observations, but might be a factor for observations needing a very flat background (much flatter than +/-0.1 e-/pixel) or

very accurate background determination. These subtraction errors due to non-linearity could be corrected in CALWF3 by adding a correction table or correction equation, where the correction would depend on FLASHCUR and FLASHDUR.

We suspect that the background may be slightly tilted when these post-flash reference files are applied to science data. This is because we used highly exposed images to model the light distribution, but actual post-flashes will have small numbers of electrons and will experience significant charge trapping during readout. Hence, our reference files are probably most accurate near the readout amplifier, but will tend to over-subtract counts in regions far from the readout amplifier (i.e. many rows distant from the amplifier in the Y coordinate direction). At this point the size of the error is not known, but is probably of order one electron. In the future this effect should be studied. It might be corrected by stacking large numbers of 12 e-/pixel flashes, modeling the result, and correcting the reference files accordingly. However, no correction is likely to be perfect, since the effect depends directly on the image background, and not on the post-flash. In situations where sky background contributes significantly, the correction would not be accurate. An alternate strategy would be to leave the post-flash reference files unchanged, and instead use pixel-based CTE corrections on the images.

Similarly the traps and bright pixels which appear in the stacked FLASH=12 image (Figure 3, Figure 4, and Figure 5) do not appear in the reference file. But again these are likely to be highly dependent on the circumstances of the science image (sky background, targets in the image, etc.), and probably these features should not be corrected through the post-flash reference file. The traps and bright pixels might also be time-dependent, and proper correction might require periodic updates to the post-flash reference files. The traps and bright pixels are generally small features, and can be eliminated through suitable dithering and stacking of the science images.

The data quality arrays have been set to zero, since there are no bad pixels specific to the post-flash calibration. However, when CALWF3 computes the value of MEANFLSH it uses the entire reference file, and hence it includes the over-scan regions of the 4206x2070 pixel format which are set to zero. Hence the value of MEANFLSH is too low by a factor of about (4096*2051)/(4206*2070)=0.9649 or about 3.5% too low. This could be corrected by setting the data quality arrays in the over-scan region to some non-zero value, and this should probably be done in some future revision to the reference files. Alternatively, CALWF3 could be modified to compute MEANFLSH while excluding the over-scan region. Our understanding is that MEANFLSH is not used for anything, so the error is relatively unimportant.

As we have seen, the post-flash brightness is unstable at the ~1.2% RMS level on timescales

of weeks. For a typical image with FLASH=12 this implies a subtraction error of ~0.14 e-/pixel and a resulting background non-uniformity of +/-0.03 e-/pixel. This is not likely to be important for science images, and hence we do not see the brightness instability as a significant issue.

The long-term stability of the post-flash should be monitored. Aging of the LED lamp will likely cause it to dim at some point (though the results so far show no significant change).The small-scale light pattern could also change if dust spots move or appear / disappear on the detector window. Large-scale changes in the illumination pattern could also appear as a result of contamination, or gross changes in the optical alignment of the instrument.

A second post-flash LED is available on "side-2" of the instrument. This could be used if the first LED failed, though this might require extensive re-calibration of the instrument on side-2. Conversely, a change-over to side-2 (e.g. due to some other instrument failure) would likely require re-calibration of the post-flash capability.

Summary

We have discussed the Phase II implementation of the post-flash capability, as well as its utilization for Cycle 20 science. Approximately 1/3 of the science exposures requested post-flash (as of the Cycle 20 Phase II deadline). The most popular value was 8 e-/pixel, but values 3, 5, 7, 9, 10, 11, 12, 15, and 20 were also used. Nearly all the programs used the LOW current setting with un-binned data; only one program used the MEDIUM current setting, and one other requested 2x2 binning.

Seven calibration proposals were briefly summarized: 12802, 13069, 13073-13076, and 13078. Using these data we briefly explored and summarized properties of the post-flash. The illumination pattern appears to be relatively uniform; broad patterns are present with +/-20% brightness variations. Stacking a large number of FLASH=12 images reveals numerous traps and interesting features comprised of bright single pixels with darks tails. Highly exposed flash images (~7000 e-/pixel) show small numbers of few-pixel dust spots, scratches, and other normal CCD features at the 10% to 30% level.

Flash images obtained on the A and B shutters are very similar. Shutter B produces flash images that average about 7% fainter than shutter A. The ratio of shutter A / shutter B flash images also shows a smooth ~4% gradient running from amplifier A to amplifier D.

The total counts/pixel appears to be non-linear with flash duration for both the LOW and MEDIUM current settings. The count rates at both current settings run about 8% higher at short flash durations as compared to 100 sec durations. The cause of this is unknown, but is probably related to the flash electronics or commanding.

We discuss the implementation of post-flash calibration in CALWF3 and the calibration pipeline, and summarize the relevant data header parameters. Calibration reference files are derived in both shutters for the LOW and MEDIUM current settings and un-binned data. These are extensively tested, and delivered to the calibration database (CDBS). The reference files are listed in Table 8.

We examine the long-term stability of the post-flash brightness. We see no evidence for long-term dimming of the LED lamp between August 2012 and June 2013. There are however, quasi-random fluctuations of the brightness with a ~1.2% RMS on timescales of weeks. The amplitude of the fluctuations appears smaller on short timescales -- shutter A & B data taken on the same orbits are correlated, and the RMS brightness fluctuation on 1-day intervals is ~0.6%. There appear to be no significant changes in the spatial illumination pattern between August 2012 and May 2013 exceeding ~0.1%.

We thank Megan Sosey for providing information on the inner workings of CALWF3, and Merle Reinhart for providing a table of all Cycle 20 GO science exposures. Finally we thank Susana Deustua for reviewing and giving helpful comments on this report.

References

Anderson, J., Mackenty, J., Baggett, S., and Noeske, K., 2012, "The Efficacy of Post-Flashing for Mitigating CTE-Losses in WFC3/UVIS Images," unpublished white paper.

Baggett, S., and Wheeler, T., 2012, "WFC3/UVIS TV3 Post-flash Results," TIR WFC3 2012-01.

Gilliland, R., Rajan, A., and Deustua, S., 2010, "WFC3 UVIS Full Well Depths, and Linearity Near and Beyond Saturation," ISR WFC3 2010-10.